Available online at www.sciencedirect.com

ScienceDirect

Procedia CIRP 40 (2016) 492 – 497

www.elsevier.com/locate/procedia

13th Global Conference on Sustainable Manufacturing - Decoupling Growth from Resource Use

Determination of displacements on a cutting disc during sawing process

Ismail Ucun[a], Fatih Onur Hocaoglu[b], Sukru Gorgulu[c]*

[a]*Afyon Kocatepe University, Technical Education Faculty, Machine Dept, Afyonkarahisar, 03200, Turkey*
[b]*Afyon Kocatepe University, Engineering Faculty, Electrical Eng.Dept, Afyonkarahisar, 03200, Turkey*
[c]*Anadolu University, Engineering Faculty, Electrical & Electronics Eng. Dept, Eskisehir, 26555, Turkey*

* Corresponding author. Tel.: +90-505-369-5454 ; fax: +90-222-321-9501. *E-mail address:* sgorgulu@anadolu.edu.tr

Abstract

In this paper, the displacement signals of a saw disc during cutting of square shaped metallic profiles are examined. The most important aspects of the study for sustainable manufacturing are reducing maintenance costs by preventing tool damage and ensuring the continuation of production by avoiding interruptions. Analysis of lateral displacements during cutting process can help controlling the cutting and circular speeds of the disc to prevent any possible damage. An experimental setup is built to collect lateral displacements. During experiments, square shaped metallic profiles are cut with different cutting parameters. The displacement signals are measured by a laser based electronic system and a detailed time-frequency analysis of the data is performed to determine the frequency components carrying significant information about the cutting process.

© 2016 The Authors. Published by Elsevier B.V. This is an open access article under the CC BY-NC-ND license (http://creativecommons.org/licenses/by-nc-nd/4.0/).

Peer-review under responsibility of the International Scientific Committee of the 13th Global Conference on Sustainable Manufacturing

Keywords: Cutting disc; lateral displacement; signal processing; Fourier transform; frequency analysis

1. Introduction

Circular saw blades/discs have been widely used to cut metal materials and they have a very important position in the industry. During cutting operations, some negative conditions such as fractures, cracks, deformations may occur in the circular saw discs. Initial contact and outputting moments of circular saw disc are vital and undesirable conditions such as vibrations and displacements occur in those moments. These undesired conditions can cause the disc to be unusable or can negatively affect the safety of the process. Therefore, it is very important to determine these factors on time [1-4]. The major goal of this study is to analyze the first contact and outputting moments of the circular saw blade by using the lateral displacement signals. In this way, especially in the case of overload, cutting and circular speeds of the disc can be reduced to prevent any possible damage. In terms of sustainable manufacturing, the continuation of the production is ensured and maintenance costs are reduced by controlling the cutting machine.

Generally, there are two parameters that can be altered in a cutting process. 1- The circular velocity (rotation speed) 2- The patial speed of the disc while cutting the material. Aslantas et al. [5] investigated axial forces acting on a segment diamond cutting disc while cutting marble. In their study, power consumptions, cutting forces and axial displacements were determined for different cutting parameters. In another study, Carmignani et al. [6] analyzed the vibrations occurred on a cutter disc. They argued that it should be possible to minimize the vibrations by altering the circular velocity of the disc. Li and Guan [7] applied time-frequency analysis to determine the fractures of cutting disc during milling operation. In their study, they proposed an efficient algorithm that consists of wavelet-based de-noising, discrete time-frequency analysis and Fast Fourier transform. Bhattacharyya et al. [8] predicted the real wears occurred on cutting disc during milling operation using cutting force signals. They applied linear filtering, time-domain averaging and wavelet transform techniques. The conclusion of their study showed that it is possible to determine the wears observed on cutting discs by selecting appropriate signal processing tools. Yesilyurt [9] used scologram and frequency analysis to determine the fault occurred on the cutting tool. For the analysis, he used vibration data that he measured and collected from the cutting tool. He observed that the vibrations occurred in cutting process were changed by alteration of feed

2212-8271 © 2016 The Authors. Published by Elsevier B.V. This is an open access article under the CC BY-NC-ND license (http://creativecommons.org/licenses/by-nc-nd/4.0/).
Peer-review under responsibility of the International Scientific Committee of the 13th Global Conference on Sustainable Manufacturing
doi:10.1016/j.procir.2016.01.112

rate. In another study, Ko and Altıntaş [10] constituted a time-domain model for milling operation. They determined the vibrations and cutting forces due to different cutting parameters using amplitude-frequency graphics via signal processing techniques. Gigardin et al. [11] examined tool fracture and wear by using rotational frequency analysis in metal cutting process. Their study showed that rotational frequency analysis should be used successively to control the wear and fracture of milling tools.

As exemplified above, there are a remarkable number of studies about analyzing the cutting force data [12-15]. Furthermore, there are other studies about analyzing the current, voltage, noise data, in addition to determining the wears and fracture on cutting disc [16-23]. In those studies, small cutting tools have been used in general. As distinct from these studies in a recent paper, Ucun et al. [24] used a bigger cutting disc having 350 mm diameter and applied signal processing techniques to determine lateral displacements occurred in the during metallic profile cutting process.

In this paper, lateral displacements occurred during cutting processes having different cutting parameters are determined using common signal processing techniques. At first, various experiments with different circular velocity and spatial cutting speed parameters are performed as mentioned in Sect. 2. Then, lateral displacements occurred during the cutting process are measured with a laser device. In Sect. 3, the collected data are analyzed in frequency domain using the developed algorithm. In Sect. 4, the frequencies carrying important information about the cutting process are determined, and the data is analyzed in time and frequency domains at the same time to determine the time intervals in which displacements changes its behavior. Consequently, the effects of cutting parameters on displacements are discussed. In Sect. 5, analysis results are listed briefly.

2. Experimental Procedure

An experimental setup is built having a computer controlled cutting machine. Schematic illustration of the setup is given in Fig. 1. The diameter of cutting disc was 350 mm whereas the radius of inner hole was 30 mm. The thickness of the disc was 3 mm. A 180 mm flange is used to stabilize the disc. Dry cutting experiments are performed.

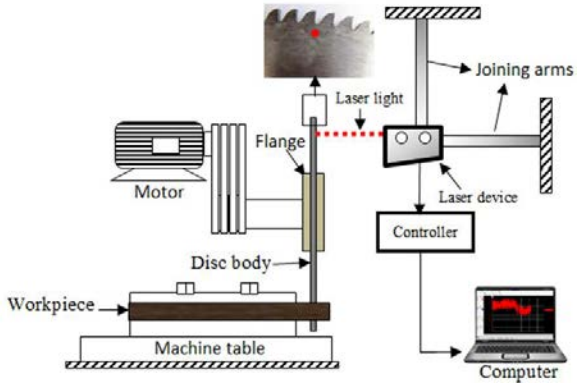

Fig. 1. Schematic illustration of cutting machine.

The disc is linked to an electric motor with rated power of 7.5 KW with a belt mechanism. Displacement measurements in cutting disc are handled by a laser device (KEYENCE) with maximum resolution of 55000 samples per second and measuring precision of 0.25µm. The measured signals are transferred to the computer with a controller circuit. The laser device was fixed to prevent the vibrations of the motor in the machine. Various experiments are performed by altering the cutting speeds and circular velocities as given in Table 1.

Table 1. Cutting parameters used in experiments.

Experiment Number	Cutting Speed, V_f (m/min)	Circular Velocity, V_c (m/s)
1	0.4	30
2	0.5	30
3	0.6	30
4	0.4	35
5	0.5	35
6	0.6	35
7	0.4	40
8	0.5	40
9	0.6	40

The displacements occurred during the experiments are illustrated in Fig. 2. $-\varepsilon_z$ and $+\varepsilon_z$ shows the distance measured by the laser displacement device. Negative sign denotes the disc is moving away and positive sign denotes the disc is approaching to the laser device. The point "p" depicted in Fig. 2 is the reference point. In each measurement, laser device assumes this point to be zero. In this way, accuracy of the measures are assured. The material cut in experiments is made from AISI 1020 steel. 25x25 mm square shaped metallic profile is cut at each experiment. The thickness of the profile was 1.5 mm. The dimensions of cutting disc teeth and metallic profile are illustrated in Fig. 3.

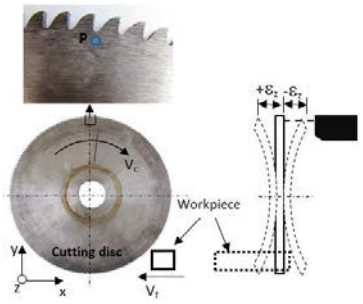

Fig. 2. Illustration of lateral deflections on the cutting disc.

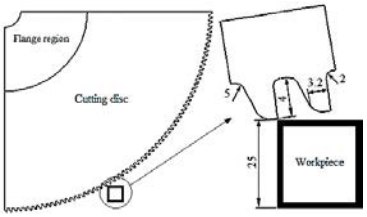

Fig. 3. Geometrical properties of the disc and the metallic profile (unit mm).

3. Short-Time Fourier Transform

J. B. Fourier developed an alternative representation for continuous-time signals in 1968 [25] which was later called as Fourier transformation (FT) and it became a powerful tool for signal-processing society. FT is theoretically defined for infinite-length continuous-time signals. However, in real-life applications, only a small portion of the signal can be held as digital samples at an instance. Under this reality, the discrete Fourier transform (DFT) is developed as the Fourier representation of finite-length discrete signals. DFT of a signal can be explicitly computed by powerful algorithms such as Fast Fourier Transform (FFT) and it plays a core role in a wide variety of signal-processing applications. DFT is used to together with various tools such as windowing and block processing to approximately find Fourier representations of signals and as seen in Fig. 4.

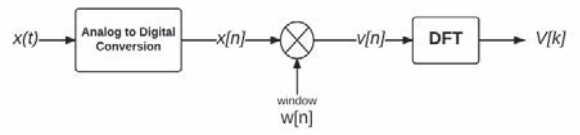

Fig. 4. A block diagram of DFT of a signal

In DFT, A sampled signal sequence $x[n]$ is to be windowed by $w[n]$ or zero-padded by either two sides to prevent the edge frequency scratches prior to transformation. As a result, the windowed/zero-padded sequence $v[n]$ doesn't have unexpected transitions at junctures when spliced to itself. $v[n]$ is then transformed as defined in Eq. 1.

$$V[k] = \sum_{n=0}^{N-1} v[n] e^{-j\left(\frac{2\pi}{N}\right)kn}, k = 0,1, \dots \dots . N-1 \quad (1)$$

where N is the length of DFT. $V[k]$ corresponds to N equally spaced samples of the Fourier transform of $v[n]$. The spacing between DFT frequency bins is $2\pi/N$, therefore the frequency spectrum is sampled with an N–point DFT. A smaller value of N may cause misleading results and a large value of N brings computational costs to the process. Therefore the optimum value for N is selected upon the frequency resolution requirements of the corresponding application.

In practical applications of signal models, the properties of a signal change in time in terms of amplitudes, frequencies, and phases. Therefore, a one-time DFT estimation is not sufficient to describe such signals. That led to the concept of time-dependent Fourier transform, also referred to as the Short-Time Fourier Transform (STFT). In the STFT representation, the 1-D sequence $x[n]$, a function of a single discrete variable, is transformed into a 2-D function of the discrete-time variable n, and discrete frequency variable $\lambda_k = 2\pi k/L$. Specifically, we define

$$X[n,k] = X[n,\lambda_k) = \sum_{m=0}^{L-1} x[n+m]w[m]e^{-j\lambda_k m}, \quad k = 0,1,\dots,N-1 \quad (2)$$

Then $X[n,k]$ is the DFT of the windowed sequence $x[n+m]w[m]$. For $m = 0,1,\dots,L-1$ and $w[m] \neq 0$, the use of window in Eq. 2 leads to the interpretation of the sampled time-dependent Fourier transform as the DFT of the windowed sequence beginning with sample n. To simplify the implementation, the sequence $x[n]$ can be separated into L-length blocks with the window position moving in jumps of R samples each time.

$$X_r[k] = X[rR,k] = X[rR,\lambda_k] = X\left[rR,\frac{2\pi k}{N}\right] = \sum_{m=0}^{L-1} x[rR+m]w[m]e^{-j\left(\frac{2\pi}{N}\right)km} \quad (3)$$

where r and k are integers such that $-\infty < r < \infty$ and $0 \leq k \leq N-1$. This notation denotes explicitly that the sampled STFT is simply a sequence of N-point DFT's of the windowed signal segments $x_r[m] = x[rR+m]w[m]$ where $-\infty < r < \infty$ and $0 \leq m \leq L-1$ with the window position in jumps of R samples in time. An illustration of STFT is presented at Fig. 5 for clarity. The inverse transform relations are not included here, since they are not used in our study. However, interested readers can head to ref. [26] for further readings.

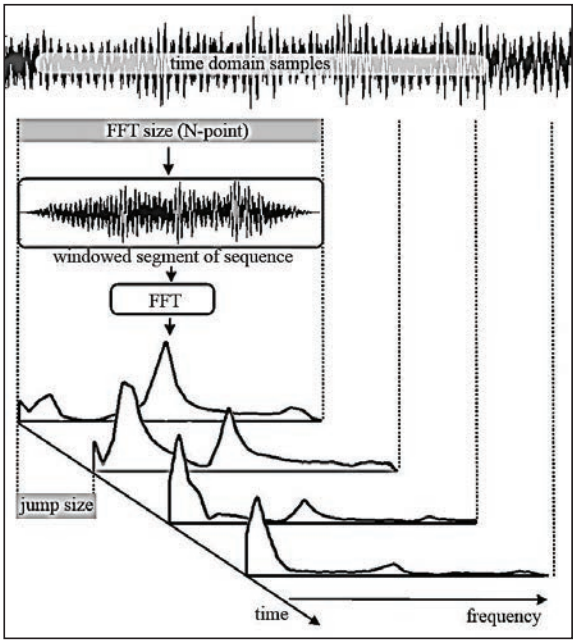

Fig. 5. A visual illustration of STFT

Many practical algorithms employ similar processes to interpret computed results and place them onto reality. In this study, STFT is employed to analyze and understand frequency information of the process of a cutting disc.

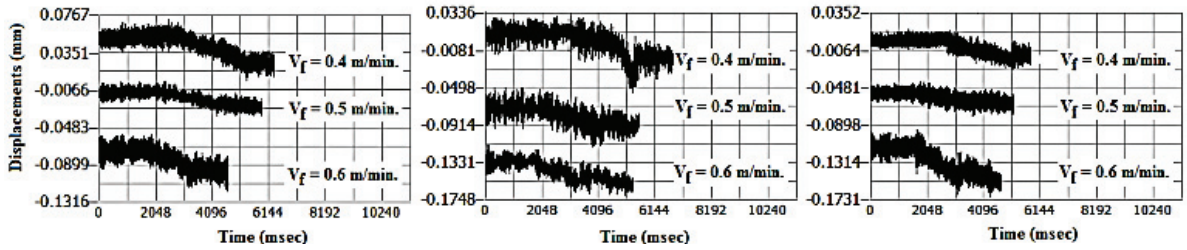

(a) (b) (c)

Fig. 6. Frequency-amplitude graphics for different cutting speed and circular velocities (a=30 m/s, b=35 m/s, c= 40 m/s).

4. Results and Discussion

4.1. Determination of lateral displacements

Fig. 6 shows time-displacement graphs of the measured and recorded data during experiments. All displacement values are negative which indicate that the cutting disc is getting closer to laser device. The variations of measured data feature a specific behavior, however it is difficult to extract this behavior within time domain. Therefore the signal is analyzed using STFT tool to determine the frequency properties of cutting process.

4.2. Signal process analysis

For deeper analysis of the data, following algorithm is developed and applied: Given that the sampling rate is 1000 samples per second, data sequence has frequency harmonics up to 500 Hz according to the Nyquist criteria. When the STFT is employed, block length L is set as 256. Each block is windowed by a tapered cosine function prior to transformation and to compensate the window-related suppression, 50% overlapping ratio is required. Therefore, jump size R is set to half of L such that each windowed sequence block shares 128 samples with previous and next blocks, implying an overlap-ratio of 50%. At a sampling rate of 1000 Hz, FFT-size L = 256 implies that the Fourier interval [-500 Hz, 500 Hz] is sampled by 256 equally spaced discrete point. Each block represents 256 milliseconds (ms) of data. The jump size R = 128 implies the Fourier analysis is repeated per 128 ms within a window length of 256 ms. FFT of each block is saved as one row (or column) of the 2-D STFT matrix. The size of this matrix depends on total number of data samples. For example, for a 6000-sample sequence with 256-point FFT size and 128-point jump-size, the number of cascaded and %50-overlapping blocks can be calculated as 45 and STFT matrix size is 256 x 45 and each element of this matrix is a complex number by the definition in Eq. 3.

The STFT matrix includes both negative and positive frequency components [-500 Hz to +500 Hz]. A bunch of operations are applied to this complex STFT matrix to make major changes of frequency visible on the graphical view. First, a real-valued magnitude matrix of size 256x45 is created by getting magnitudes. Second, magnitudes in the matrix are square-rooted twice and normalized to make smaller and bigger values closer. Third, the matrix is filtered by a two-dimensional 3x3 median filter to make relatively minor changes disappear and form a smooth view. Then this matrix is used to create a 2D view. Once this matrix is formed; time intervals and frequencies are represented by a 2-D plane and corresponding amplitudes are represented as negative-intensities (darker areas denote higher amplitudes) on this time-frequency plane as illustrated in Fig. 7. The resulting graph is actually a modified version of spectrogram of data.

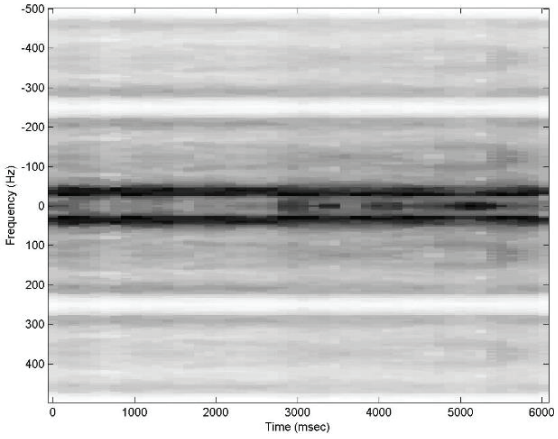

Fig. 7. A modified spectrogram of data (for Experiment 1)

It can be observed from the graphical image, that displacements can be analyzed by examining some specific frequencies. However, occurrence times are not clear. To determine the exact times of displacements, lower-frequency [0 to +256 Hz] bins are summed together. It is clear from the figures that each graphic includes four different frequency extremes. These frequency extremes point beginning times cutting states of disc given in Table 2. In state 1, disc is turning by a predetermined speed without cutting anything. In state 2, cutting operation starts. In state 3, cutting operation goes on and finishes. In state 4, the cutting process finished and there occurs a friction between the profile and lateral side of the disc.

Table 2. Cutting states of the disc.

Cutting states			
1	2	3	4
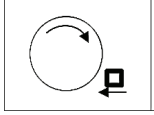	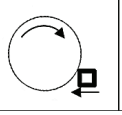	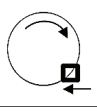	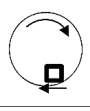

The random behavior of the signal corresponds to 1st state. In this state the disc starts turning free without touching the profile. The sudden increase at the magnitude of frequency corresponds to 2nd state indicates first contact of the disc to the metallic profile. After this sudden change, the disc enters into the profile and the alteration of the frequency shows a stable behavior (3rd state) for a while until cutting finishes. When cutting process finishes, the profile moves away from the disc and a sudden frequency change occurs again. This time corresponds to the end of the cutting process (4th state). On the other hand, since the disc generates oscillations while revolving around it, local frequency extremes occur during 1st state. Furthermore, similar local extremes are observed during third state by the effect of friction between cut portion of the profile and lateral side of the disc.

To determine the start and end point of the cutting process the behavior of low frequency component summations are examined for each experiment as illustrated in Fig. 9. In these figures start and finish points of the cutting process are labeled and illustrated by CS and CF, respectively. Since the data accusation from each experiment are independent, corresponding CS and CF times are different. The time between CS and CF is shortened by increasing the cutting speed. The frequency values at the first contact are lowered. However, the frequency values are higher at finishing times. When the profile leaves the cutting disc, it becomes free and frequency values increase, considerably.

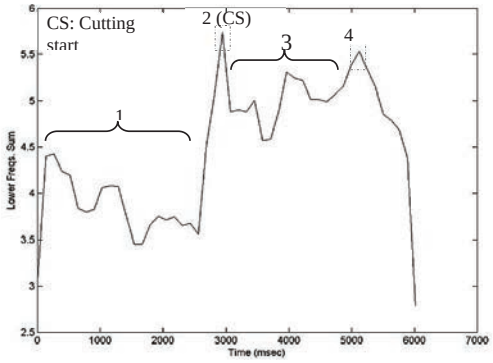

Fig. 8. Amplitudes of the sum of low frequencies versus time.

The alteration of frequencies depending on cutting speed and circular velocities are illustrated at Fig. 9. These figures include whole cutting process. The exact times in which the cutting process is begun and finished are shown at these figures. The determined starting and finishing times are different for each experiment due to different cutting speeds. For 30 m/s circular velocity case, higher amplitudes of low-frequency are observed at the first contact. When the cutting disc penetrates into the

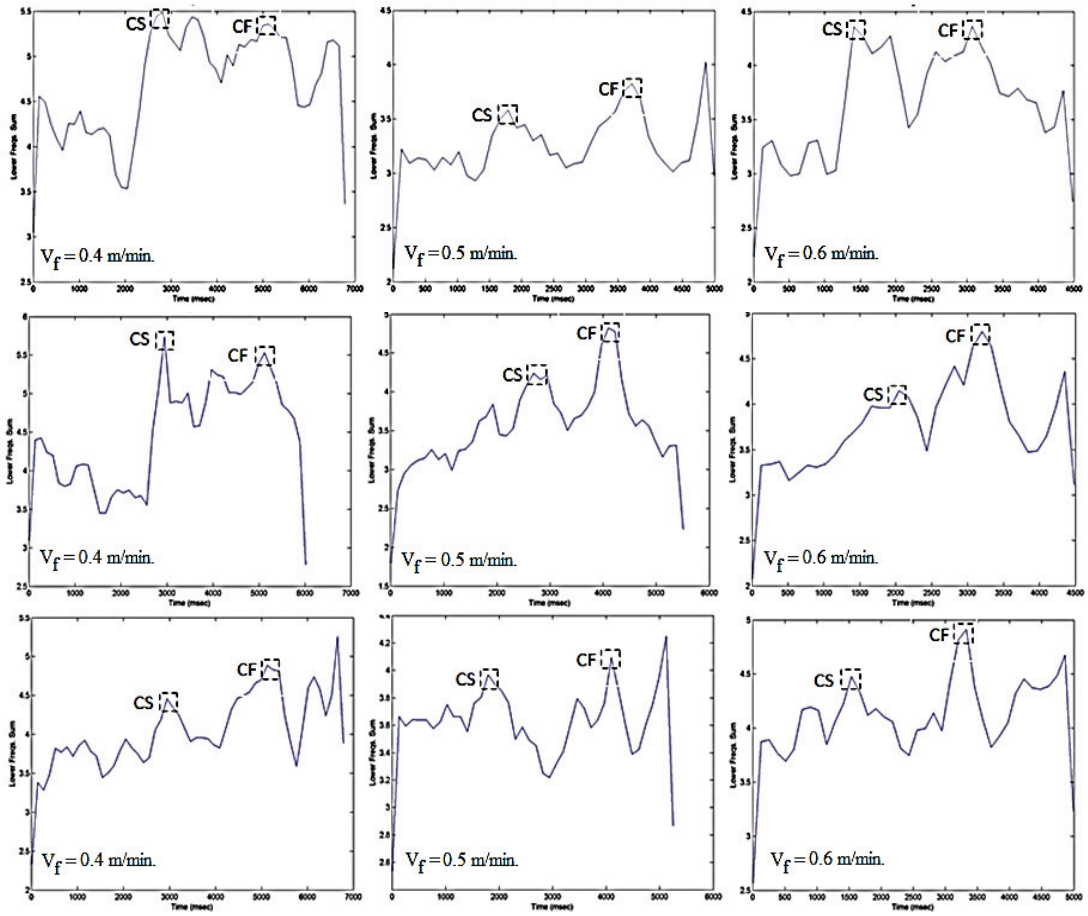

Fig. 9. Sum of low frequencies versus time for different cutting speed and circular velocities (up 30 m/s, middle 35 m/s, bottom 40 m/s).

profile with a higher cutting speed, the magnitude of the low frequencies are increased. The oscillations of the disc are absorbed by the effect of friction for higher cutting speed. When the cutting speed is increased to 0.5 m/min from 0.4 m/min, it is observed that the amplitude of the low frequencies is decreased. By increasing the circular velocity (to 40 m/s) lower frequency values are increased. On the other hand, the amplitude of the frequency is reduced when the cutting disc penetrated into the metallic profile by the effect of friction for higher cutting speeds. It is obtained from the experiments that, the amplitude of the frequency is higher at the end of the cutting process than the amplitude of the frequency during the process. This is because of two facts that the cutting disc turns to one side only. And at the end of the cutting process, friction between one side of the profile and the disc continues for a while. Finally, the cutting disc becomes free and the amplitude of the frequency increases considerably.

5. Conclusion

Alterations of lateral displacements for different cutting parameters are determined in this study. It is not possible to clearly understand the dynamic behavior of the temporal data directly. However, after applying STFT, it was possible to understand and interpret the process by using the spectrogram. Increasing the cutting velocity caused an increase at lower frequency amplitude values. This means lateral displacements of the disc are increased. At circular velocity values such as 35 and 40 m/s, the amplitude values have an unstable behavior. From the beginning of an initial touch of the disc to the profile, it is obtained that, amplitudes of frequency components increases, considerably. This situation indicates that vibrations of the disc are increased. Furthermore, when the profile is under the cutting process, amplitude of higher frequency components are decreased. Near the end of the cutting process low frequency components are generally lower then high frequency ones. By separation of the cut profile from the disc, amplitudes of lower frequency components gets higher since the disc becomes free and some local extreme occur for a while.

The study shows analysis of frequency features during different stages of the metal cutting process. One can determine exact times of states using real-time analysis and control the circular and cutting speeds of disc to prevent tool damages using the methods described in the paper. Such a control can help preventing tool damages. As a result maintenance costs can be reduced and production interruptions can be avoided in terms of sustainable manufacturing.

Acknowledgements

This study is a part of the research project with ID#112M347 supported by TUBITAK (The Scientific and Technological Council of Turkey). We thank our colleagues who provided insight and expertise that greatly assisted the research.

References

[1] Ucun İ. Aslantaş K., Büyüksagiş İ.S., Taşgetiren S., 2012, Micromechanical modelling of diamond debonding in composite segments, Journal of Theoretical and Applied Mechanics, 50, 2, 609-626.
[2] Ucun İ, 2012, Investigation of effect on lateral displacement and forces of cutting mode in sawability of metal profile using cutting disc, Trans. of the Can. Soc. for Mech. Eng., 36, 1, 37-47.
[3] Tönshoff H.K., Jendryschik J., 1985, Dynamical behavior of disk like rotating tools, Computers & Struc., 21, (1/2), 203-211.
[4] Ucun İ, Colakoğlu M, Taşgetiren S., 2008,Crack initiation and growth in circular saw, J. of Theoretical and Applied Mechanics, 46, 2, 291-303.
[5] Aslantaş K., Özbek O., Ucun İ., Büyüksağiş İ.S., 2009, Investigation of the effect of axial cutting force on circular diamond sawblade used marble cutting process, Materials and Manufac. Processes, 24, 1423-1430.
[6] Carmignani C., Forte P., Rustighi E., 2006, Experimental simulation of the sharpening process of a disc blade and analysis of its dynamic response, Journal of Sound and Vibration, 297, 649-663.
[7] Li X., Guan X.P., 2004, Time-frequency-analysis-based minor cutting edge fracture detection during end milling, Mech. Systems and Signal Process, 18, 1485-1496.
[8] Bhattacharyya P., Sengupta D., Mukhopadhyay S., 2007, Cutting force based real time estimation of tool wear in face milling using a combination of signal processing techniques, Mech. Systems and Signal Process, 21, 2665-2683.
[9] Yesilyurt İ., 2006, End mill breakage detection using mean frequency analysis of scalogram, Int. J. of Mach. Tool & Manu. 46, 450-458.
[10] Ko J.H., Altıntaş Y., 2007, Time domain model of plunge milling operation, Int. J. of Mac. Tool & Manufac. 47, 1351-1361.
[11] Gigardin F., Remond D., Rigal J.F., 2010, Tool wear detection in milling–An original approach with a non-dedicated sensor, Mech. Systems and Signal Process, 24, 1907-1920.
[12].Sze Y.K., Lee W.B., Cheung C.F., To S., 2006, A power spectrum analysis of effect of rolling texture on cutting forces in single-point diamond turning, Journal of Material Processing Tech., 180, 305-309.
[13] Ramulu M., Kim D., Choi G., 2003, Frequency analysis and characterization in orthogonal cutting of glass fiber reinforced composites, Composites : Part A, 34, 949-962.
[14] Lin S.C., Lin R.J., 1996, Tool wear monitoring in face milling using force signals, Wear, 198, 136-142.
[15] Ertunc H.M., Oysu C., 2004, Drill wear monitoring using cutting force signals, Mechatronics, 14, 533-548.
[16] Shao H., Wang H.L., Zhao X.M., 2004, A cutting power model for tool wear monitoring in milling, Int. J. of Mach. Tools & Manufac, 44, 1503–1509.
[17] Kopac J., Sali S., 2001, Tool wear monitoring during the turning process, Journal of Material. Process. Tech, 113, 312-316.
[18] Liu X., Cheng K., 2005, Modelling the machining dynamics of peripheral milling, Int. J. of Mach. Tool & Manufac, 45, 1301-1320.
[19] Li X., Dong S., Yuan Z., 1999, Discrete wavelet transform for tool breakage monitoring, Int. J. of Mach. Tool & Manufac, 39, 1935-1944.
[20] Kalvoda T., Hwang Y.R., 2010, A cutter tool monitoring in machining process using Hilbert-Huang transform, Int. J. of Mach. Tool & Manufac, 50, 495-501.
[21] Braun S., Rotberg J., Lenz E., 1987, Signal processing for single tooth milling monitoring, Mech. Systems and Signal Process, 1, 2, 185-196.
[22] Tansel İ., Trujillo M., Nedbovyan A., Velen C., Bao W.Y., Arkan T.T., Tansel B., 1998, Micro-end-milling-III. Wear estimation and tool breakage detection using acoustic emission signals, Int. J. of Mach. Tool & Manufac, 38, 1449-1466.
[23] Min B. K., O'neal G., Koren Y., Pasek Z., 2002, Cutting process diagnostics utilising a smart-cutting tool, Mech. Systems and Signal Process, 16, 475-486.
[24] Ucun I., Hocaoglu F. O., Gorgulu S., 2011, A time-frequency analysis for deflection of a cutting disc used in sawing process, Advanced Materials Res., 268-270, 847-852.
[25] Oppenheim A.V., Willsky A.S., Young I.T. 1997, Signals and systems, Prentice-Hall, Englewood Cliffs, New Jersey, pp. 180-250.
[26] Oppenheim A.V., Schafer R.W., Buck J.R.. 1999, Discrete-time Signal Processing, 2nd Ed. Prencite-Hall, Upper Saddle River, pp. 71